



Cite this: *Mater. Adv.*, 2025, 6, 8157

Benign-by-design synthesis of covalent triazine-imidazolium networks under room temperature aqueous conditions for CO₂ utilization

Niloofer Abbasi,^a Piero Mastorilli,^b Stefano Todisco^b and Mojtaba Khorasani^{ID, *ac}

In this study, we have described that the nucleophilic aromatic substitution reaction between a hydroxyl-tagged imidazolium and cyanuric chloride in a mixture of water and acetone as a reaction medium at room temperature leads to the formation of a new series of imidazolium-based covalent triazine frameworks (CTFs). The material denoted as I-CTF-1 was identified as a family of nitrogen-rich cationic polymers. The influence of polar solvents, including pure DMSO and its aqueous solutions, as well as the presence of ionic surfactants, such as CTAB or SDS, on the textural properties of the synthesized cationic CTFs has been examined. The elemental analysis indicated that the polymerization occurred meticulously, as evidenced by the strong correlation between the theoretical and experimental loading values of imidazolium and triazine groups. ¹³C CP-MAS NMR confirmed that both triazine and imidazolium groups are incorporated into the CTF network. The presented CTF was thermally stable until 300 °C. I-CTF-1 also exhibited an interesting CO₂ adsorption capacity of 2.2 mmol g⁻¹. This catalyst displayed excellent activity toward direct coupling of carbon dioxide with various types of terminal epoxides under 1 mol% catalyst, and 10 bar CO₂ at 80 °C. It could be recycled at least 4 times without any remarkable decrease in its activity or selectivity.

Received 6th June 2025,
Accepted 29th September 2025

DOI: 10.1039/d5ma00604j

rsc.li/materials-advances

Introduction

Recently, the development of functionalized covalent organic polymers has garnered significant interest owing to their wide-ranging application in various fields such as gas separation, energy storage, electronic devices, and catalysis.^{1,2} The organic compositions of these materials facilitate the efficient diffusion of organic substrates to the catalytic sites and allow for a typically high loading of catalysts.^{3,4} The covalent triazine frameworks (CTFs) or triazine-based covalent organic polymers represent a vital subgroup of covalent organic polymers, classified as polymer networks that possess aromatic triazine functional groups.^{5,6} Triazine groups can provide the possibility for the coordination of metal cations.⁷ It has been also well-documented that the presence of triazine groups greatly enhances the adsorption capacity of CO₂, making CTF an outstanding candidate for applications related to CO₂ capture or conversion.^{8–10} The process of synthesizing covalent triazine frameworks is usually categorized

into two fundamental strategies: the construction of triazine units or the incorporation of triazine components.^{6,11} The first method typically includes nitrile trimerization under ionothermal conditions, while the second strategy involves the integration of triazine derivatives into the CTF framework by means of various chemical bonds.¹¹ Utilizing these approaches has allowed the development of CTFs with desirable characteristics, which makes them suitable for various applications. The choice of synthesis conditions plays a crucial role in determining the final properties of the CTFs, which subsequently influences their effectiveness in catalytic applications.¹² Most importantly, green chemistry fundamentally prioritizes the development of CTFs by reducing environmental impact, minimizing energy consumption, utilizing solvent-free approaches or safe solvents, and employing cost-effective reagents and catalysts, while still achieving high efficiency.

Imidazolium cations with halide as a counter ion are one of the highly eco-sustainable classes of organocatalysts for the production of cyclic carbonates through the direct coupling of CO₂ and epoxides.^{13–20} The cyclic carbonates are extensively used as polar aprotic solvents, as intermediates in pharmaceuticals, and in polymer design.²¹ It is believed that this strategy not only plays a significant role in minimizing CO₂ emissions but also supports the integration of renewable resources into chemical synthesis.²² To date, to allow the recovery and reuse of the imidazolium catalyst, various types of polymer network

^a Department of Chemistry, Institute for Advanced Studies in Basic Sciences (IASBS), Zanjan 45137-66731, Iran. E-mail: m_khorasani@iasbs.ac.ir; Fax: +98-24-33153232; Tel: +98-24-33153223

^b DICATECH Department, Politecnico of Bari, via Orabona, 4 70125 Bari, Italy

^c Research Center for Basic Sciences & Modern Technologies (RBST), Institute for Advanced Studies in Basic Sciences, IASBS, Zanjan 45137-66731, Iran



have been used for the immobilization of the imidazolium catalyst for CO_2 cycloaddition to the epoxides.^{23–28} It is well-documented that by incorporating imidazolium groups into a solid polymer network that is modified with electron-donating or hydrogen bond donor groups, we can significantly boost the activity of the imidazolium catalyst through a synergistic effect.^{29–31} On the other hand, recent advancements have revealed that in addition to the presence of triazine groups, the CO_2 capture capacity of CTFs can be enhanced by incorporating CO_2 -philic groups, including N-heterocyclic moieties.^{32,33} The aforementioned features can be collectively pictured in the decorated CTFs with imidazolium groups (Im-CTFs), which have recently drawn substantial attention in the area of carbon dioxide conversion reactions. Im-CTFs are typically synthesized through the direct trimerization of imidazolium linkers tagged by nitrile groups.^{34–39} The direct trimerization of imidazolium derivatives containing nitrile groups at elevated temperatures or in the presence of superacids results in the formation of imidazolium-based CTFs with a high porosity that show considerable promise for a range of applications, especially in areas that demand materials with large surface areas, including catalysis and gas storage.^{40,41} However, the dehalogenation and graphitization processes that occur for the prepared CTF layers at elevated temperatures likely result in a decrease of both halide and nitrogen content within this specific type of CTF.^{34,42} These limitations might be particularly problematic in the context of imidazolium precursors with iodide ions, which are notably susceptible toward oxidation. In response to these restrictions, some research efforts have been redirected to the synthesis of cationic CTFs through the incorporation of triazine components, utilizing the reaction between imidazolium precursors and triazine derivatives. Zhong *et al.* described the synthesis of an organic polymer based on imidazolium and triazine through the Sonagashira reaction, utilizing suitable monomers in the presence of palladium and copper catalysts at 100 °C in DMF as the solvent.⁴³ Wen and co-workers have reported the synthesis of the imidazolium-based porous triazine polymer by the Debus–Radziszewski reaction of 1,3,5-(4-aminophenyl)triazine, formaldehyde and glyoxal at 80 °C.⁴⁴ Recently, Van der Voort *et al.* introduced an imidazopyridinium-based covalent organic framework (COF) with triazine units by a two-step strategy through first imine-COF formation with a picolinaldehyde derivative and an appropriate amine and then cyclization of the picolinaldehyde-dimine parts of the COF intermediate.⁴⁵ While the aforementioned methods present intriguing possibilities, they also face significant challenges, including the requirement for elevated temperatures, the risk of dehalogenation, the necessity of expensive metal catalysts, and the reliance on high-cost precursors. The $\text{S}_{\text{N}}2$ substitution reaction between suitably modified substrates comprising imidazole and triazine groups at higher temperatures has also emerged as an effective route for the synthesis of imidazolium-triazine-based covalent organic polymers.^{46–50} Huang and co-workers have described how a supramolecular porous ionic network can be prepared using the direct quaternization of 2,4,6-tris-imidazolyl-1,3,5-triazine with cyanuric chloride, followed by hydrolysis and *in situ* assembly.⁵¹ One-pot base-mediated synthesis

of the nitrogen-rich ionic porous network *via* nucleophilic substitution and quaternization of *H*-imidazole with cyanuric chloride under basic conditions at 80 °C has been introduced by Pan and co-workers.⁵² In light of the straightforward nature of the above processes, it appears that the simplest technique for synthesizing imidazolium-based CTF materials is the incorporation of triazine through nucleophilic substitution reactions. However, the direct attachment of imidazolium cations to the triazine units has caused electron deficiency of the triazine rings, an issue that may limit their potential application in CO_2 adsorption capacity. Therefore, the synthesis of cationic CTFs under ambient conditions by using readily available precursors while the triazine ring has electron-donating groups still faces some challenges.

In 1959, Allan and Allan described that the 2,4,6-tris(4-formylphenoxy)-1,3,5-triazine derivatives can be prepared in nearly quantitative yield by the dropwise addition of an aqueous solution of sodium phenoxide to a solution of cyanuric chloride in acetone at room temperature.⁵³ Although several COFs or CTF precursors have been synthesized using this methodology, so far, to the best of our knowledge, there is no report on the synthesis of any cationic CTF or related polymers by using this simple reaction.^{6,11} Therefore, we decided to use this strategy for the synthesis of a new series of cationic CTFs by using the direct reaction of homemade aryl imidazoliums tagged by hydroxyl functional groups with commercially available cyanuric chloride (Scheme 1). The advantages of this method include adopting mild reaction conditions, the use of readily available imidazolium precursor, and using aqueous solution as a green chemical environment. This strategy also avoids the necessity for high temperatures, precious metal catalysts, or expensive precursors. This approach is notably distinct from previous studies, as it involves the direct integration of electron-donating groups into the triazine rings, thereby endowing them with properties that enhance their interaction with CO_2 . We have also investigated the impact of solvent and ionic surfactants during the synthesis of Im-CTFs, emphasizing the significance of ambient conditions. The final materials were employed as recoverable organocatalysts for direct coupling of carbon dioxide with various types of epoxides under mild reaction conditions.

Experimental section

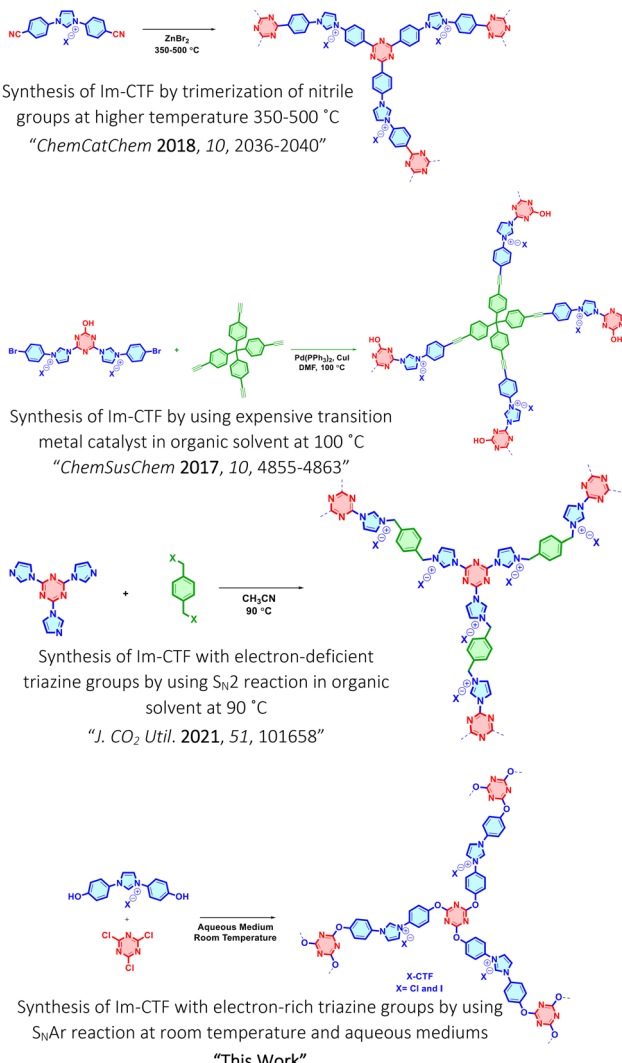
Synthesis of *N*¹,*N*²-bis(4-hydroxylphenyl)ethane-1,2-diimine

A 30 mL round-bottom flask was charged with 4-aminophenol (5.46 g, 50 mmol), glyoxal (3.4 mL, 30 mmol, 40% in water), and 70 mL of 2-propanol. To this mixture, a few drops of acetic acid were added as a catalyst. The reaction was conducted at 40 °C for 24 hours. The solid product was collected *via* filtration and subsequently washed with 2-propanol and diethyl ether, yielding *N*¹,*N*²-bis(4-hydroxylphenyl)ethane-1,2-diimine (5.02 g, 20.9 mmol, 84% yield).⁵⁴

Synthesis of 1,3-bis-(4-hydroxyphenyl)imidazolium chloride (BHPICl)

A round-bottom flask was charged with 30 mL of ethyl acetate and heated in an oil bath to a temperature of 70 °C. To this,





Scheme 1 The general pathways for the synthesis of Im-CTF.

*N*¹,*N*²-bis(4-hydroxylphenyl)ethane-1,2-diimine (5.0 g, 20.8 mmol) and paraformaldehyde (0.687 g, 22.9 mmol) were added. After approximately 30 minutes, during which all solids dissolved completely, the dropwise addition of a trimethylsilyl chloride (TMSCl) solution (1.9 g, 600 μ L, 17.46 mmol) in ethyl acetate (354 μ L) was performed. The mixture was stirred for 2 hours at 70 °C and then cooled in a refrigerator at 4 °C overnight. Following this, the reaction mixture was vacuum filtered and washed with ethyl acetate, resulting in a brown powder (4.8 g, 80% yield).⁵⁴

Synthesis of 1,3-bis(4-hydroxyphenyl)imidazolium iodide (BHPII)

1,3-Bis(4-hydroxyphenyl)imidazolium chloride (0.5 g, 1.5 mmol) was dispersed in 8 mL of deionized water. After deoxygenation through argon gas bubbling, the mixture was sonicated for 10 minutes. A saturated potassium iodide (2.0 g, 12.0 mmol) solution in deionized water was then added gradually, and the mixture was stirred at room temperature for 8 hours under an argon environment. The resulting solid was

washed several times with deionized water and acetone, followed by drying under vacuum at 60 °C overnight.

Synthesis of Cl-CTF

A mixture of 1,3-bis(4-hydroxyphenyl)imidazolium chloride (0.519 g, 1.8 mmol) and sodium hydroxide (140 mg, 3.5 mmol) was prepared by dissolving them in a 20 mL solution of acetone and water (v/v = 1 : 1) while stirring in an ice bath. Subsequently, a solution of cyanuric chloride (0.221 g, 1.2 mmol) in 10 mL of acetone was added dropwise to the flask. Following a reaction period of 6 hours, 50 mL of distilled water was introduced into the reaction mixture and the resulting solid was collected through filtration and was first washed with dilute sodium bicarbonate solution and then multiple times with water and acetone to yield 0.555 g of Cl-CTF (91% yield).

Synthesis of I-CTF-1

The procedure for synthesizing Cl-CTF was adopted, except that 1,3-bis(4-hydroxyphenyl)imidazolium iodide (0.684 g, 1.8 mmol) was used. Finally, 0.720 g (93%) of I-CTF-1 was obtained. The iodide ion content was quantified using Andrew's titration method. In this procedure, a pre-weighed I-CTF-1 catalyst was added to a mixture of carbon tetrachloride and hydrochloric acid, and subsequently titrated with a potassium iodate standard solution. The endpoint of the titration was determined by the disappearance of the violet coloration associated with free iodine.

Direct coupling of epoxides with CO₂ catalyzed by I-CTF-1

A stainless steel high-pressure reactor was charged with epoxide (5 mmol) and I-CTF-1 (0.024 g, 1 mol%). The reactor was then gradually pressurized to 10 bar, and the reaction mixture was stirred at 80 °C for the specified duration. After the required time, the mixture was allowed to cool to ambient temperature, followed by a slow depressurization of the reactor. Subsequently, 5 mL of ethyl acetate was added to facilitate the separation of the catalyst from the reaction mixture. The supernatant was collected and analyzed *via* gas chromatography, utilizing trimethylbenzene (TMB) as the internal standard. Further purification was achieved through column chromatography using a solvent mixture of ethyl acetate and *n*-hexane (1 : 5). All products were verified using ¹H- and ¹³C-NMR and FTIR spectroscopy.

Reusability of I-CTF-1 during the coupling of epichlorohydrin with CO₂

After the first runs as mentioned above, I-CTF was carefully washed with dichloromethane (2 \times 10 mL) and hot ethanol (2 \times 10 mL) and then dried under vacuum overnight. The catalyst was then employed exactly as in the first run.

Results and discussion

The imidazolium linkers tagged by hydroxyl groups were prepared through a two-step process, beginning with *p*-amino phenol and glyoxal, followed by the formation of the imidazolium ring in the presence of paraformaldehyde and trimethylsilyl

chloride. With an emphasis on the CTF synthesis under ambient temperature, subsequently, the synthesis of the corresponding X-CTFs was achieved through the stoichiometric reaction of homemade imidazolium linkers with commercially available cyanuric chloride in various solvents to yield X-CTFs, where X denotes the counter ions associated with the imidazolium groups. We first investigated the role of the reaction medium in synthesizing the related CTFs. In a water:acetone (1:2) mixture as the solvent, I-CTF-1 was synthesized. The obtained CTF was first characterized by nitrogen physisorption analysis to gain more information about its porosity. I-CTF-1 exhibited a type IV isotherm and H₃ hysteresis loop according to the IUPAC classification (Fig. 1a).⁵⁵ The surface area was found to be 27 m² g⁻¹, indicating that the related CTF is a nonporous polymer. It is worth noting that immediately after the addition of a homogeneous solution of imidazolium linker to the transparent cyanuric chloride solution, a new solid was observed. Therefore, fast and irreversible polymerization of the precursor leads to a highly packed solid network with low porosity. These observations may be related to the fact that the formed aromatic C–O bond is strong with a length of 1.37 Å and a bond energy of 460 kJ mol⁻¹, which forms completely unidirectionally very quickly and does not allow the formation of the expected layered structures with a high surface area.⁵⁶ However, I-CTF-1 was insoluble in typical organic solvents such as THF, DMAc, DMSO, NMP, and DMF, indicating the presence of covalently cross-linked networks. In the next step, we have investigated the role of the addition of DMSO as a polar aprotic solvent to the aqueous acetone medium. We expected that DMSO would prevent fast polymerization and lead to CTFs with a higher surface area. In this regard, I-CTF-2 was synthesized while the mixture of water:acetone:DMSO was used as the reaction medium (see SI for details). Unfortunately, I-CTF-2 also had a low surface area of

11 m² g⁻¹ (Fig. S1). Even the stepwise addition of DMSO did not have an effect, and the resulting I-CTF-3 with a surface area of 17 m² g⁻¹ was achieved (Fig. S2). We also found that no CTF was obtained in dry DMSO alone as a reaction medium. Recently, surfactant-assisted synthesis of COFs and CTFs has been described for the preparation of COFs or CTFs with a high surface area.^{57–61} The imidazolium precursor under the initial basic conditions has a negative charge and when its polymerization proceeds, its surface changes to positively charged due to the presence of imidazolium groups. In this regard, the effect of two ionic surfactants, cetyltrimethylammonium bromide (CTAB) and sodium dodecyl sulfate (SDS), to improve the surface area of CTFs has been studied. We found that I-CTF-4 in a very low reaction yield can be obtained if CTAB was first added to an aqueous acetone solution containing I-imidazolium precursor and NaOH. Besides the low reaction yield, I-CTF-4 still shows a low surface area of 24 m² g⁻¹ (Fig. S3). A similar result was also observed for I-CTF-5 with a low surface area of 22 m² g⁻¹ in which SDS as an anionic surfactant was used instead of CTAB (Fig. S4). It seems that in our CTF system, the fast and irreversible formation of C–O bonds can be explained by both thermodynamic and kinetic factors. The C–O bond has a high bond dissociation energy, so its formation is energetically favourable. After these bonds are formed, they strengthen the polymer backbone and make it highly rigid and resistant to reverse reactions. This strong thermodynamic stability likely causes the appearance of dense, cross-linked networks with a low surface area, instead of porous layered structures. On the other hand, the polymerization proceeds *via* irreversible nucleophilic aromatic substitution (S_NAr), where the activation energy for C–O bond formation is sufficiently low under our reaction conditions.⁶² This leads to rapid chain propagation and minimal opportunity for defect healing or rearrangement, emphasising the formation of tightly packed structures. Also, because the formation of C–O bonds is not well-oriented, it does not promote growth in two dimensions and stacking between layers, which can suppress the overall porosity. Additionally, the lack of reversible steps limits the formation of extended open networks, favouring compact morphologies. Additionally, the process was found to be independent of medium polarity or surfactants. This means that the fast polymerization of CTF precursors does not rely on ionic surfactant preorganization or polar environments to create porous structures. We found that under identical reaction conditions for I-CTF-1, if the imidazolium precursor with chloride ions (BHPICl) was used, again a dense and nonporous polymer denoted as Cl-CTF with a surface area of 22 m² g⁻¹ was obtained (Fig. 1b). I-CTF-1 and Cl-CTF were selected from the described CTFs for more detailed characterization and catalyst testing, thanks to their simple preparation technique. Scanning electron microscopy (SEM) analysis and energy dispersive X-ray spectroscopy (EDS) were performed to examine the morphology and elemental distribution of I-CTF-1 and Cl-CTF. Both CTFs exhibited an aggregated spherical morphology with particle diameters of about 500 nm (Fig. 1c and d). The EDS maps of I-CTF-1 confirmed that all expected elements, such as nitrogen, carbon, oxygen, and iodine, were homogeneously

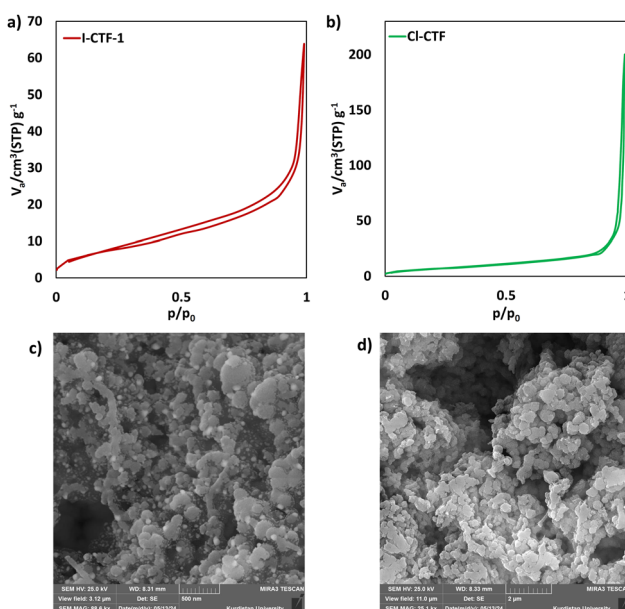


Fig. 1 Nitrogen adsorption–desorption isotherms for (a) I-CTF-1 and (b) Cl-CTF and SEM images for (c) I-CTF-1 and (d) Cl-CTF.



distributed in the sample (Fig. 5S). The absence of chloride ions in this sample rules out any possible exchange of chloride ions coming from the reaction of cyanuric chloride hydroxyl-tagged imidazolium precursor. All expected elements were also observed in the EDS elemental mapping of Cl-CTF (Fig. S6).

The presence of functional groups and related bonds in the synthesized CTFs was further revealed by Fourier transform infrared (FTIR) spectroscopy. The sharp peaks at 1550 cm^{-1} are assigned to the stretching vibration of $\text{C}=\text{N}$ in imidazolium and triazine rings (Fig. 2a and b). The FTIR data also confirm a high polymerization degree for the related CTFs due to the disappearance of the peaks assigned to $\text{C}-\text{Cl}$ of triazine and OH in the imidazolium precursors. The sharp peaks around 1490 cm^{-1} can also be assigned to $\text{C}=\text{C}$ of the aromatic rings in the imidazolium precursors. The incorporation of cationic imidazolium groups was further confirmed by zeta potential analysis (Fig. 2c and Fig. S7). The surface potentials for I-CTF-1 and Cl-CTF were found to be 48 and 29 mV; these findings are in good agreement with the results of FTIR. Despite a low surface area, I-CTF-1 could adsorb the unusual amount of 2.2 mmol g^{-1} CO_2 under a pressure of 1 bar at room temperature (Fig. 2d). The higher adsorbent capacity of I-CTF-1 can be related to the high density of imidazolium and electron-rich triazine groups in the sample. To assess the thermal stability of

Table 1 CHN results and loading of imidazolium groups for the synthesized CTFs

Materials	%C	%N	C/N ^a	Im ^b [mmol g ⁻¹]	TA ^c [mmol g ⁻¹]	Im/TA ^d
I-CTF-1	41.9	11.9	4.1 (4.2)	2.1 (2.3)	1.4 (1.5)	1.5 (1.5)
Cl-CTF	45.6	14.1	3.7 (4.2)	2.5 (2.9)	1.7 (1.9)	1.5 (1.5)
Re-I-CTF-1	42.5	11.8	4.2 (4.2)	2.1 (2.3)	1.4 (1.5)	1.5 (1.5)

^a Experimental C/N molar ratio calculated from %C and %N. The values in parentheses indicate the theoretical C/N molar ratio derived from the theoretical formula of $(\text{C}_{51}\text{H}_{33}\text{N}_{12}\text{O}_6\text{X}_3)_n$. ^b The experimental loading of imidazolium groups was calculated using $(10 \times \%N)/(14 \times 4)$. The values in parentheses indicate the theoretical loading of imidazolium groups. ^c The experimental loading of triazine rings was calculated from %N and the equation of $(10 \times \%N)/(14 \times 6)$. The values in parentheses indicate the theoretical loading of triazine groups.

^d Experimental imidazolium to triazine molar ratios in CTFs, which are in good agreement with theoretical values (number in parentheses).

both CTF catalysts, thermogravimetric analyses (TGA) were performed under a nitrogen atmosphere (Fig. 2e and f). Two samples demonstrated a similar weight loss of approximately 2 to 8% occurring below $100\text{ }^\circ\text{C}$, which is attributed to the desorption of water and solvents that were retained within the structures of the organic network of the CTFs. Despite the organic nature of the CTFs, the main weight loss of both CTFs begins at $350\text{ }^\circ\text{C}$, confirming the high thermal stability of the samples. These findings prove the formation of the organic network from cyanuric chloride and imidazolium precursors. The results of elemental analysis for both CTFs showed a good relation between theoretical and experimental calculations (Table 1). By considering the formula of $(\text{C}_{51}\text{H}_{33}\text{N}_{12}\text{O}_6\text{X}_3)_n$ for both CTFs, where X is chloride or iodide ions, a theoretical carbon to nitrogen molar ratio (C/N) of 4.2 was estimated for both CTFs. The experimental C/N molar ratio was found to be 4.1 and 3.7 for I-CTF-1 and Cl-CTF, respectively. These data confirm a good co-polymerization of the CTF precursors. From the observed nitrogen content and using the equation of $(10 \times \%N)/(14 \times 4)$, the loading of imidazolium groups was estimated to be 2.3 and 2.9 mmol g⁻¹ for I-CTF-1 and Cl-CTF, respectively, in very close to those from theoretical calculations. The loading of triazine groups was also estimated for both CTFs, which was in good agreement with the theoretical calculations. More importantly, both the theoretical and experimental molar ratio of imidazolium to triazine rings was found to be 1.5 for I-CTF-1 and Cl-CTF, a finding clearly confirming that the polymerization process was complete. The loading of iodide ions of I-CTF-1 was found to be 2.1 mmol g^{-1} by Andrew's titration, which was in agreement with the CHN calculation.

The X-ray photoelectron spectroscopy (XPS) survey of I-CTF-1 established the presence of carbon, nitrogen, iodide, and oxygen in the catalyst (Fig. 3a). The C 1s XPS spectrum was fitted to three peaks at approximately 284.8 eV, 286.2, and 288.1 eV (Fig. 3b). The first peak corresponds to $\text{C}=\text{C}$ and $\text{C}-\text{C}$ bonds. The middle peak can be assigned to $\text{C}=\text{N}$ bonds in both the triazine and imidazolium units. The last peak is associated with the $\text{C}-\text{O}$ bond. The N 1s spectrum was also deconvoluted into two peaks (Fig. 3c). The peak at a lower binding energy of 399.5 eV is attributed to the nitrogens of the triazine nodes,

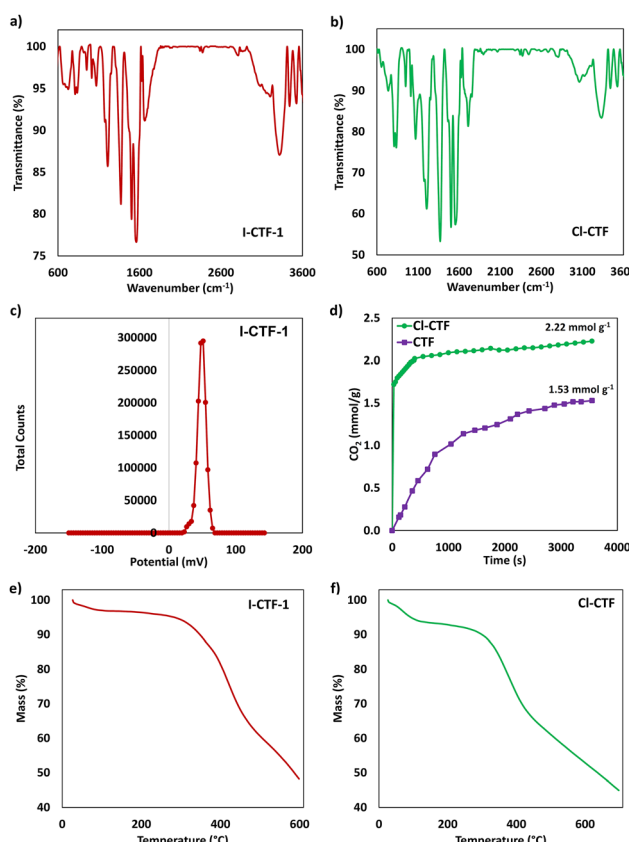


Fig. 2 FTIR spectra for (a) I-CTF-1 and (b) Cl-CTF. (c) Zeta potential curve for I-CTF-1. (d) CO_2 adsorption capacity (1 bar CO_2 at room temperature) for Cl-CTF and CTF (CTF without imidazolium units). TG pattern for (e) I-CTF-1 and (f) Cl-CTF.



while the peak at a higher binding energy of 402 eV relates to electron-deficient nitrogens in the imidazolium rings of the linker. The peaks corresponding to iodide ions appeared as two distinct peaks at 618.3 eV and 629.8 eV, with a doublet separation of 11.5 eV, which can be associated with $I\ 3d_{5/2}$ and $I\ 3d_{3/2}$, respectively (Fig. 3d). Interestingly, the absence of peaks related to chloride ions around 200 eV indicates that all chloride ions were thoroughly replaced by iodide ions. Overall, these findings support the successful polymerization of home-made imidazolium groups with cyanuric chloride. The incorporation of bis-phenyl imidazolium groups was also confirmed by cross-polarization magic-angle-spinning ^{13}C NMR (CP MAS ^{13}C -NMR) spectroscopy (Fig. 3e). All aromatic carbons could be observed with a similar pattern to its ^{13}C NMR in the liquid phase. The broad peak around 123.7 ppm can be assigned to aromatic carbons of phenylene groups. The sharp peak centered at about 132.4 ppm is related to carbons of imidazolium rings (NCHCH). The peak observed at 152.5 is correlated to the carbons bonded to oxygen atoms. The carbon ($\text{N}-\text{Mx0043};=\text{N}^+$) of the imidazolium rings was observed at 158.4 ppm. Finally, the highly deshielded carbon around 174.1 can be related to the triazine rings of I-CTF-1. These results also clearly confirmed that imidazolium and triazine rings are successfully incorporated into the network of I-CTF-1.

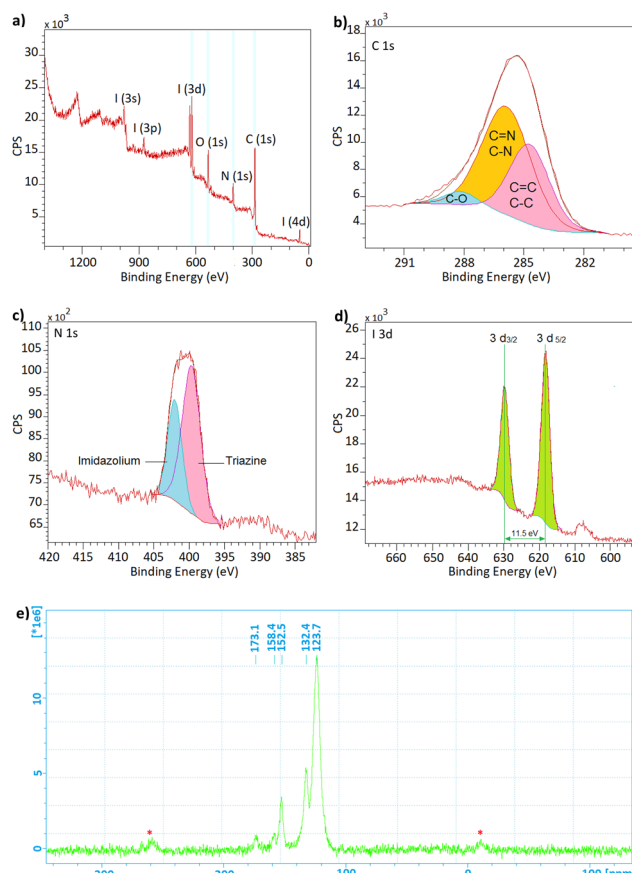


Fig. 3 XPS spectrum of I-CTF-1: (a) survey, (b) C 1s, (c) N 1s, and (d) I 3d. (e) ^{13}C CP-MAS NMR spectrum of I-CTF-1 (the peaks marked by red stars are the spinning resonance of the aromatic rings).

After the characterization of both I-CTF-1 and Cl-CTF, their activity toward the cycloaddition of CO_2 to epoxide was checked. We first focused on the I-CTF-1 catalyst. To do this, the direct coupling of epichlorohydrin (ECH) as a model substrate with carbon dioxide was investigated in a high-pressure single reactor under solvent-free conditions. The conversion of ECH was determined by gas chromatography (GC) analyses with trimethylbenzene (TMB) as a typical internal standard (Table 2). Under the conditions of 0.75 mol% I-CTF-1, with 10 bar of CO_2 at 70 °C, it was observed that only 52% of ECH was able to convert into the corresponding ECH carbonate within 5 h (Table 2, entry 1). The increase of catalyst loading to 1 mol% leads to an improvement of the reaction yield to 84% (Table 2, entry 2). The reaction yield was increased to 98% using either 1 or 1.25 mol% I-CTF, under 10 bar CO_2 at 80 °C within 5 h (Table 2, entries 3 and 4). Therefore, 1 mol% I-CTF-1 was selected for the next optimization tests. Our studies showed that a decrease in reaction time to 3 hours, while keeping all other conditions unchanged, resulted in a poor ECH conversion of 52% (Table 2 entry 5). So, the best time was found to be 5 h. The effect of CO_2 pressure was then investigated. It was found that under the lower pressures of 5 and 7.5 bar, respectively, 73 and 75% ECH conversion was observed, while ECH quantitatively transformed to the corresponding cyclic carbonate under a higher pressure of 15 bar CO_2 (Table 2, entries 6–8). Due to easy operation and safety issues, 10 bar CO_2 was selected as the best condition. Therefore, 1 mol% I-CTF, 10 bar CO_2 , 80 °C, and 5 h were established as the best reaction conditions (Table 2, entry 3). Under these conditions, 1,3-bis-(4-phenol)imidazolium iodide (BHPII) in homogeneous form just resulted in 5% yield. This result carefully highlights the importance of the vicinity of imidazolium groups and triazine

Table 2 The possible coupling of CO_2 with epichlorohydrin catalyzed by I-CTF-1 under various reaction conditions^a

Entry	Catalyst (mol%)	<i>t</i> (h)	<i>T</i> (°C)	P_{CO_2} (bar)	Yield ^b (%)	TON ^c	TOF ^d (h ⁻¹)
1	I-CTF-1 (0.75)	5	70	10	52	69	14
2	I-CTF-1 (1)	5	70	10	84	84	22
3	I-CTF-1 (1)	5	80	10	98	98	26
4	I-CTF-1 (1.25)	5	80	10	98	78	16
5	I-CTF-1 (1)	3	80	10	52	52	10
6	I-CTF-1 (1)	5	80	5	73	73	15
7	I-CTF-1 (1)	5	80	7.5	75	75	15
8	I-CTF-1 (1)	5	80	15	99	99	20
9	BHPII (1)	5	80	10	5	5	1
10	Br-CTF (1)	5	80	10	74	74	15
11	Cl-CTF (1)	5	80	10	35	35	7
12 ^e	CTF	5	80	10	3	—	—

^a Reaction conditions: epichlorohydrin (5 mmol) under the described conditions. ^b GC yield by using trimethylbenzene as the internal standard. ^c TONs were determined by (mmol of product)/(mmol of halide).

^d Turnover frequency calculated by TON/time (h). ^e 20 mg of catalyst without imidazolium units denoted as CTF was used (see SI for details).



in the solid network of I-CTF-1 for CO_2 conversion. It is well-documented that the nature of the halide ion plays a critical role in the mentioned CO_2 conversion. To further elucidate this, we performed comparative reactions using Cl-CTF and Br-CTF (see SI for details). The catalytic activity followed the trend I-CTF-1 > Br-CTF > Cl-CTF, which correlates well with the known nucleophilicity and leaving group tendencies of halide ions under solvent-free conditions (Table 2, entries 10 and 11). Notably, this trend is consistent with our recent reports, further validating the structural design strategy employed for I-CTF-1.⁶³ To experimentally confirm the role of imidazolium groups with iodide ions in catalytic activity, we synthesized a structurally analogous covalent triazine framework lacking imidazolium units, referred to as CTF. This control material exhibited a significantly lower CO_2 adsorption capacity of 1.5 mmol g⁻¹ compared to Cl-CTF (Fig. 2d) and a markedly reduced conversion of ECH under identical reaction conditions (Table 2, entry 12). These results strongly indicate that the presence of imidazolium rings plays a crucial role in enhancing both the CO_2 adsorption capacity and the catalytic performance.

In the second part of the catalysis studies, the potential of I-CTF-1 for the synthesis of cyclic carbonates with different epoxides has been explored (Table 3). Despite highly reactive ECH, other epoxides needed a slightly longer reaction time to obtain excellent conversion. The short-chain aliphatic epoxides such as propylene or butylene oxide were nearly completely converted to their corresponding cyclic carbonate in good yields (Table 3, entries 1 and 2). Alkyl derivatives of glycidols also underwent conversion to the related cyclic carbonates, resulting in nearly quantitative yields (Table 3, entries 3–6). Butyl glycidyl carbonate could be furnished from its epoxide in excellent yield under the optimized reaction conditions (Table 3, entry 3). Phenyl glycidyl carbonate, an effective monomer for the synthesis of polycarbonates, serves as an alternative to caprolactam for application as a suture thread and can be selectively synthesized using the catalytic protocol we have presented (Table 3, entry 4). It is noteworthy that glycidyl ether derivatives, which possess functional groups that are sensitive to oxidation or polymerization, such as allyl glycidyl or glycidyl methacrylate ethers, were selectively transformed into their cyclic carbonates without any indication of side reactions (Table 3, entries 5 and 6). The presented catalyst also exhibited excellent results toward styrene oxide, considered a relatively sluggish terminal epoxide, resulting in a 92% yield under the described reaction conditions. Unlike the previously discussed terminal epoxides, cyclohexene oxide, classified as a less-reactive internal epoxide, yielded only 10% conversion to the corresponding cyclohexene carbonate. This was observed despite increasing the catalyst loading to 2 mol% and raising the reaction temperature to 100 °C (see Table 3, entry 8). In the next stage, regarding the higher stability of Cl-based catalysts under oxidizing conditions for long times, we also checked the activity of the Cl-CTF catalyst for the title CO_2 cycloaddition reaction (Table S1). After checking various parameters, it was found that by using ECH as a model substrate, 3 mol% Cl-CTF and 10 bar CO_2 at 100 °C are the best reaction

Table 3 Substrate scope for the synthesis of 5-ring cyclic carbonates catalyzed by I-CTF^a

Entry	Epoxide	Time (h)	GC yield ^c (%)	TON ^d
1		15	98	98
2		24	97	97
3		24	98	98
4		24	97	97
5		24	98	98
6		24	98	98
7		24	92	92
8		24 ^b	>10	5

^a Reaction conditions: epoxide (5 mmol), I-CTF-1 (24 mg, 1 mol%) and CO_2 pressure (10 bar) at 80 °C unless otherwise stated. ^b 2 mol% I-CTF-1 at 100 °C. ^c GC yield by using trimethylbenzene as the internal standard.

^d TONs were determined by (mmol of product)/(mmol of iodide).

conditions (Table S1, entry 4). We also found that the already studied epoxides were selectively coupled with CO_2 under the described reaction conditions (Table S2).

We also investigated the possible recovery of I-CTF-1 during the direct coupling of CO_2 with ECH under the described reaction conditions in entry 3 of Table 2. After the first run, the catalyst was collected from the reaction medium, washed several times with hot ethanol and dichloromethane, and dried under a vacuum overnight. The catalyst was used for another run. We found that I-CTF-1 could be recycled for at least 4 reaction cycles without any remarkable decline in its activity or selectivity (Table S3). As anticipated, the recovered catalyst displayed an isotherm identical to that of the fresh catalyst, given that I-CTF-1 itself lacked porosity (Fig. S8). Elemental analysis confirmed that the composition of the catalyst did not undergo any alteration, and the content of carbon and nitrogen was found to be 42.5 and 11.8%, respectively (Table 1, entry 3). Consistent with the findings from CHN analysis, TGA exhibited a similar weight loss pattern for the recovered catalyst compared to the fresh catalyst, suggesting that the catalyst's composition remained stable throughout the catalytic processes and did not decompose into its constituent monomers (Fig. S9).

Although our presented I-CTF-1 or Cl-CTF exhibited a low surface area, they showed excellent activity toward the cycloaddition of CO_2 to epoxides under relatively mild reaction

conditions. To provide perfect insights, their activity has been compared with that of some similar supported imidazolium-based catalysts in terms of catalyst textural properties and the required reaction conditions. The activity of the presented catalyst clearly parallels that of catalysts derived from mesoporous organosilica materials, which include imidazolium catalysts with iodide ions previously reported by our group (Table S5). Our catalyst was also compared to recent catalysts built by incorporating imidazolium groups into the CTF, COF, and POP. It is inferred from these comparisons that the presented catalyst exhibited similar activity to the selected catalytic systems. Our catalytic system could be operated with slightly higher loading amounts of catalyst but at much lower temperatures, whereas most of the compared catalysts have been optimized to use lower loading of catalyst at higher temperatures. The high activity of the presented catalyst under relatively mild reaction conditions was reflected in its organic nature as well as its multi-functionality. The organic nature of the catalyst allows the organic substrate to diffuse easily into the network of the catalyst where halide ions as catalytic centers are located. In light of the chemistry of CTFs embedded with imidazolium functionalities, and considering recent experimental and computational studies, we propose a plausible reaction mechanism that underscores the synergistic interaction between the triazine core and imidazolium ring. Density functional theory (DFT) calculations, *in situ* FTIR spectroscopy, and experimental data collectively demonstrate that the triazine ring behaves as a Lewis base, engaging with the electrophilic carbon center in CO₂.^{40,46,48} This interaction promotes the spatial localization of CO₂ near the imidazolium-rich domains of the framework, enhancing adsorption efficiency. Moreover, while the halide counter ions of imidazolium act as Lewis bases and actively participate in epoxide ring-opening reactions, the imidazolium moiety itself contributes to enhanced CO₂ adsorption through dipole–quadrupole interactions.⁶⁴ The resulting synergy between the closely packed imidazolium groups and electron-rich triazine motifs within the organic framework not only improves the mass transport of organic substrates and local CO₂ enrichment but also facilitates efficient CO₂ activation. This concerted mechanism significantly enhances the catalytic performance of halide ions in the chemical fixation of CO₂ under relatively mild reaction conditions. For illustrative clarity, the proposed mechanism and interplay are schematically represented in Fig. S14.

Conclusion

In summary, the effect of the reaction media and the presence of ionic surfactants on the textural properties of a series of imidazolium-based covalent triazine frameworks with iodide ions (I-CTF) at room temperature has been investigated. It was found that in the absence of ionic surfactants, both aqueous DMSO or acetone solution led to nonporous and high-density imidazolium-triazine-based polymeric networks with an excellent reaction yield. However, SDS or CTAB as an ionic surfactant

could not improve the textural properties of the resulting CTFs. However, the presented catalyst was found to be an active catalyst for CO₂ cycloaddition of a variety of terminal epoxides into their corresponding five-membered cyclic carbonates. Despite the low surface area of the I-CTF catalyst, it was comparable to previously reported imidazolium-based catalysts with CTF families for the title reaction. The significant loading of imidazolium groups alongside electron-rich triazine units promotes the CO₂ adsorption capacity of the I-CTF catalyst. These features demonstrate an enhancement in the catalytic performance attributed to the co-supported iodide ions.

Author contributions

N. A.: investigation, conducting experiments, data curation, and validation. S. T. and P. M.: solid phase NMR analysis. M. K.: conceptualization, validation, data curation, writing the original draft, and supervision.

Conflicts of interest

There are no conflicts to declare.

Data availability

The data supporting this article have been included as part of the Supplementary information (SI). Supplementary information: Experimental details for the synthesis of all reference catalysts; ¹H- and ¹³C-NMR as well as FTIR spectra of all organic compounds; the results of FT-IR, nitrogen adsorption–desorption isotherms, and TGA for the reference catalysts and reused catalysts. See DOI: <https://doi.org/10.1039/d5ma00604j>.

Acknowledgements

The authors acknowledge IASBS Research Councils for supporting this work. This work is based on research funded by Iran National Science Foundation (INSF) under project no. 4040929. The authors gratefully acknowledge Prof. Ahad Ghaemi from IUST for performing carbon dioxide adsorption capacity studies.

References

- 1 M. S. Lohse and T. Bein, *Adv. Funct. Mater.*, 2018, **28**, 1705553.
- 2 R. Liu, K. T. Tan, Y. Gong, Y. Chen, Z. Li, S. Xie, T. He, Z. Lu, H. Yang and D. Jiang, *Chem. Soc. Rev.*, 2021, **50**, 120–242.
- 3 Y. Zhang and S. N. Riduan, *Chem. Soc. Rev.*, 2012, **41**, 2083–2094.
- 4 J. Guo and D. Jiang, *ACS Cent. Sci.*, 2020, **6**, 869–879.
- 5 M. Liu, L. Guo, S. Jin and B. Tan, *J. Mater. Chem. A*, 2019, **7**, 5153–5172.
- 6 S. E. Peter, P. Thomas, P. Vairavel and N. A. V. Kumar, *Mater. Adv.*, 2024, **5**, 9175–9209.
- 7 Y. Ren, S. Yang and Y. Xu, *Acc. Chem. Res.*, 2025, **58**, 474–487.



8 G. Liu, S. Liu, C. Lai, L. Qin, M. Zhang, Y. Li, M. Xu, D. Ma, F. Xu, S. Liu, M. Dai and Q. Chen, *Small*, 2024, **20**, 2307853.

9 R. Kishan, P. Rani, G. Singh and C. M. Nagaraja, *Cryst. Growth Des.*, 2024, **24**, 7878–7887.

10 H. Li, A. Dilipkumar, S. Abubakar and D. Zhao, *Chem. Soc. Rev.*, 2023, **52**, 6294–6329.

11 L. Liao, M. Li, Y. Yin, J. Chen, O. Zhong, R. Du, S. Liu, Y. He, W. Fu and F. Zeng, *ACS Omega*, 2023, **8**, 4527–4542.

12 Z. Qian, Z. J. Wang and K. A. I. Zhang, *Chem. Mater.*, 2021, **33**, 1909–1926.

13 S. Asgarloo, G. Anvarian-Asl, S. Joudian, N. Abbasi, B. Karimi and M. Khorasani, *Emergent Mater.*, 2025, **8**, 2723–2736.

14 G. Anvarian-Asl, S. Joudian, S. Todisco, P. Mastrorilli and M. Khorasani, *Nanoscale*, 2024, **16**, 16977–16989.

15 K. Guo, N. Ji, F. Han, Q. Yang, N. Wang and C. Miao, *RSC Sustainability*, 2024, **2**, 1074–1080.

16 J. D. Ndayambaje, I. Shabbir, L. Dong, Q. Su and W. Cheng, *J. Mater. Chem. A*, 2024, **12**, 11448–11462.

17 P. Miksovsky, K. Rauchenwald, S. Naghdi, H. Rabl, D. Eder, T. Konegger and K. Bica-Schröder, *ACS Sustainable Chem. Eng.*, 2024, **12**, 1455–1467.

18 W.-L. Bao, J. Kuai, H.-Y. Gao, M.-Q. Zheng, Z.-H. Sun, M.-Y. He, Q. Chen and Z.-H. Zhang, *Dalton Trans.*, 2024, **53**, 6215–6223.

19 M. Khorasani, B. Karimi and H. Vali, *React. Chem. Eng.*, 2022, **7**, 2618–2628.

20 Z.-A. Chen, L. Zou, R. Cao and Y.-B. Huang, *Natl. Sci. Rev.*, 2025, **12**, nwaf032.

21 A. J. Kamphuis, F. Picchioni and P. P. Pescarmona, *Green Chem.*, 2019, **21**, 406–448.

22 M. He, Y. H. Sun and B. X. Han, *Angew. Chem., Int. Ed.*, 2022, **61**, e202112835.

23 A. Sahoo, S. Jaiswal, S. Das and A. Patra, *ChemPlusChem*, 2024, **89**, e202400189.

24 W. Natongchai, D. Crespy and V. D'Elia, *Chem. Commun.*, 2025, **61**, 419–440.

25 K. Huang, J.-Y. Zhang, F. Liu and S. Dai, *ACS Catal.*, 2018, **8**, 9079–9102.

26 Z. Xu, W. Wang, B. Chen, H. Zhou, Q. Yao, X. Shen, Y. Pan, D. Wu, Y. Cao, Z. Shen, Y. Liu, Q. Xia, X. Li, X. Zou, Y. Wang and L. Jiang, *Chem. Commun.*, 2023, **59**, 14435–14438.

27 T. Kessaratikoon, T. Theerathanagorn, D. Crespy and V. D'Elia, *J. Org. Chem.*, 2023, **88**, 4894–4924.

28 R. Jamil, L. C. Tomé, D. Mecerreyres and D. S. Silvester, *Aust. J. Chem.*, 2021, **74**, 767–777.

29 R. Luo, X. Liu, M. Chen, B. Liu and Y. Fang, *ChemSusChem*, 2020, **13**, 3945–3966.

30 G. Li, S. Dong, P. Fu, Q. Yue, Y. Zhou and J. Wang, *Green Chem.*, 2022, **24**, 3433–3460.

31 L. Guo, K. J. Lamb and M. North, *Green Chem.*, 2021, **23**, 77–118.

32 S. Hug, L. Stegbauer, H. Oh, M. Hirscher and B. V. Lotsch, *Chem. Mater.*, 2015, **27**, 8001–8010.

33 L. Tao, F. Niu, C. Wang, J. Liu, T. Wang and Q. Wang, *J. Mater. Chem. A*, 2016, **4**, 11812–11820.

34 T.-T. Liu, R. Xu, J.-D. Yi, J. Liang, X.-S. Wang, P.-C. Shi, Y.-B. Huang and R. Cao, *ChemCatChem*, 2018, **10**, 2036–2040.

35 J. S. Lee, H. Luo, A. G. Baker and S. Dai, *Chem. Mater.*, 2009, **21**, 4756–4758.

36 G. H. Gunasekar, K. Park, V. Ganesan, K. Lee, N.-K. Kim, K.-D. Jung and S. Yoon, *Chem. Mater.*, 2017, **29**, 6740–6748.

37 S. Rajendiran, G. H. Gunasekara and S. Yoon, *New J. Chem.*, 2018, **42**, 12256–12262.

38 M.-J. Mao, M.-D. Zhang, D.-L. Meng, J.-X. Chen, C. He, Y.-B. Huang and R. Cao, *ChemCatChem*, 2020, **12**, 3530–3536.

39 P. Wu, H. Liu, M. Sun, Y. Zeng, J. Ye, S. Qin, Y. Cai, W. Feng and L. Yuan, *J. Mater. Chem. A*, 2021, **9**, 27320–27331.

40 K. Park, K. Lee, H. Kim, V. Ganesan, K. Cho, S. K. Jeong and S. Yoon, *J. Mater. Chem. A*, 2017, **5**, 8576–8582.

41 C. Yue, W. Wang and F. Li, *ChemSusChem*, 2020, **13**, 5996–6004.

42 O. Buyukcakir, S. H. Je, S. N. Talapaneni, D. Kim and A. Coskun, *ACS Appl. Mater. Interfaces*, 2017, **9**, 7209–7216.

43 H. Zhong, Y. Q. Su, X. W. Chen, X. J. Li and R. H. Wang, *ChemSusChem*, 2017, **10**, 4855–4863.

44 Y. Mao, Y. Shi, Y. Su, Q. Shen, Y. Zhang, X. Wang and X. Wen, *Green Chem.*, 2021, **23**, 5981–5989.

45 G. Matthys, A. Laemont, N. De Geyter, R. Morent, R. Lavendomme and P. Van Der Voort, *Small*, 2024, **20**, 2404994.

46 X. Fang, C. Liu, L. Yang, T. Yu, D. Zha, W. Zhao and W.-Q. Deng, *J. CO₂ Util.*, 2021, **54**, 101778.

47 T.-T. Liu, J. Liang, Y.-B. Huang and R. Cao, *Chem. Commun.*, 2016, **52**, 13288–13291.

48 K. Cai, P. Liu, Z. Chen, P. Chen, F. Liu, T. Zhao and D.-J. Tao, *Chem. Eng. J.*, 2023, **451**, 138946.

49 K. Cai, P. Liu, P. Chen, C. Yang, F. Liu, T. Xie and T. Zhao, *J. CO₂ Util.*, 2021, **51**, 101658.

50 S. Jiao, L. Deng, X. Zhang, Y. Zhang, K. Liu, S. Li, L. Wang and D. Ma, *ACS Appl. Mater. Interfaces*, 2021, **13**, 39404–39413.

51 Z.-H. Hei, G.-L. Song, C.-Y. Zhao, W. Fan and M.-H. Huang, *RSC Adv.*, 2016, **6**, 92443–92448.

52 C. Ai, X. Ke, J. Tang, X. Tang, R. Abu-Reiq, J. Chang, J. Yuan, G. Yu and C. Pan, *Polym. Chem.*, 2022, **13**, 121–129.

53 F. J. Allan and G. G. Allan, *Recl. Trav. Chim. Pays-Bas*, 1959, **78**, 375–381.

54 Y. Miki, H. Sajiki and Y. Sawama, *Synlett*, 2020, 699–702.

55 M. Thommes, K. Kaneko, A. V. Neimark, J. P. Olivier, F. Rodriguez-Reinoso, J. Rouquerol and K. S. W. Sing, *Pure Appl. Chem.*, 2015, **87**, 1051–1069.

56 F. H. Allen, O. Kennard, D. G. Watson, L. Brammer, A. G. Orpen and R. Taylor, *J. Chem. Soc., Perkin Trans. 1*, 1987, 1–19.

57 K. Liu, H. Qi, R. Dong, R. Shihhare, M. Addicoat, T. Zhang, H. Sahabudeen, T. Heine, S. Mannsfeld, U. Kaiser, Z. Zheng and X. Feng, *Nat. Chem.*, 2019, **11**, 994–1000.

58 H. Sahabudeen, H. Qi, M. Ballabio, M. Položij, S. Olthof, R. Shihhare, Y. Jing, S. Park, K. Liu, T. Zhang, J. Ma, B. Rellinghaus, S. Mannsfeld, T. Heine, M. Bonn, E. Cánovas, Z. Zheng, U. Kaiser, R. Dong and X. Feng, *Angew. Chem., Int. Ed.*, 2020, **59**, 6028–6036.

59 X. Hu, Z. Zhan, J. Zhang, I. Hussain and B. Tan, *Nat. Commun.*, 2021, **12**, 6596.

60 G.-H. Yang, Z. Zhang, C.-C. Yin, X.-S. Shi and Y. Wang, *Chin. J. Polym. Sci.*, 2022, **40**, 338–344.



61 S. Zhang, X. Wu, C. Ma, Y. Li and J. You, *J. Agric. Food Chem.*, 2020, **68**, 3663–3669.

62 T. Chen, W.-Q. Li, W.-B. Hu, W.-J. Hu, Y. A. Liu, H. Yang and K. Wen, *RSC Adv.*, 2019, **9**, 18008–18012.

63 S. Joudian, S. Todisco, P. Mastorilli and M. Khorasani, *ACS Appl. Nano Mater.*, 2025, **8**(29), 14882.

64 J. Liang, Y.-Q. Xie, X.-S. Wang, Q. Wang, T.-T. Liu, Y.-B. Huang and R. Cao, *Chem. Commun.*, 2018, **54**, 342–345.

